Engineering Structures 31 (2009) 1042–1055

Contents lists available at ScienceDirect

Engineering Structures

journal homepage: www.elsevier.com/locate/engstruct

Damage detection of a woven fabric composite laminate using a modal strain energy method

Huiwen Hu *, Jieming Wang

Composite Materials and Lightweight Structures Laboratory, Department of Vehicle Engineering, National Pingtung University of Science and Technology, Pingtung Neipu 91201, Taiwan

ARTICLE INFO

Article history:
Received 15 November 2007
Received in revised form
19 December 2008
Accepted 23 December 2008
Available online 29 January 2009

Keywords:
Woven fabric composite
Modal strain energy
Equivalent models
Experimental modal analysis
Damage index

ABSTRACT

This paper presents the detection of surface cracks in a woven fabric composite laminate using a modal strain energy method. A carbon fabric F3T-282/epoxy (DICY) is used to fabricate a plain woven laminate. In the first place, the unknown material properties are computed by utilizing an inverse method through finite element analysis and experimental modal analysis. Three equivalent models, i.e. cross-ply $[0/90]_{ns}$, orthotropic and representative cell, are established to simulate the woven laminate. Tensile tests are also performed to measure the mechanical properties for comparison. A surface crack is created to represent nominal damage which is comparatively small and does not significantly affect the global stiffness of the woven laminate. Experimental modal analysis is conducted on the woven laminate to obtain the modal displacements before and after damage. The modal displacements are used to compute the modal strain energies through the three equivalent models. A damage index is defined by employing the fractional modal strain energy of the woven laminate before and after damage, and then used to identify the location of the surface crack. Limited by grid points in measurement, a differential quadrature method is utilized to compute the partial differential terms in strain energy formula. Consequently, the damage indices obtained from global and local measurements successfully locate the surface crack in woven laminate. Only a few measured mode shapes are required in this method, which has a relatively low cost and flexibility in measurement, nondestructive evaluation, and feasibility of real-time detection in woven laminates.

1. Introduction

The application of woven fabric composites in engineering structures has been significantly increased due to attractive characteristics, such as flexible processing options, low fabrication cost, while also possessing adequate mechanical properties. Nevertheless, the crimp regions lead to considerable complexities in mechanical analysis, especially in comparison to the unidirectional fiber-reinforced composites. Although some analytical and finite element models have been successfully developed [1–6] recently, not much work has addressed the issue of failure and damage development [5,6], not to mention their detection. The damage mechanisms of woven fabric laminates are practically the same as in unidirectional fiber-reinforced composite laminates, i.e. matrix cracking, delamination and fibre fracture. Gao et al. [7] indicated that transverse matrix cracking was the first readily observable type of damage and occurred in woven fabric laminates under tensile loading. In general, damage in composite materials can be detected by nondestructive techniques such as optical microscopy, acoustic emission, radiography or hydro-ultrasonics (C-scan), especially for the small damage such as matrix cracking. Nevertheless, most of these conventional methods are time-consuming, costly, and inappropriate for large components and integrated structures.

Vibration-based methods have been increasingly adopted as tools of damage detection for composite materials due to their flexibility in measurement, cost effective approaches, and the feasibility of real-time structural health monitoring. The basic idea of these methods is to use the information of modal parameters, such as frequency, mode shape and damping ratio, to assess the structural damage. Cawley and Adams [8], Tracy and Pardoen [9] found that the natural frequencies of a composite beam are affected by the size and damage location. Salawu [10,11] concludes that the changes in natural frequency may not be sufficient for structural damage localization. Shen and Grady [12] indicated that local delamination does not have a noticeable effect on the global mode shape of composite beams, but delamination does cause irregularity of mode shapes. Kim et al. [13] used a frequency-based method and a mode-shape-based method to successfully

* Corresponding author. Tel.: +886 8 7703202; fax: +886 8 7740398.
E-mail address: huiwen@mail.npust.edu.tw (H. Hu).

0141-0296/$ – see front matter
doi:10.1016/j.engstruct.2008.12.015

locate the damage size and damage severity of the beam structures, respectively. Combining the concept of modal strain energy, this approach was applied to monitor the damage in the plate-girder bridges under uncertain temperature conditions [14].

Damping properties have seldom been used for damage detection due to their small effects on frequency variations. Curadelli et al. [15] indicated that damping changes may cause the detection of the nonlinear, dissipative effects that damages produce. A novel scheme has been proposed to detect structural damage by means of the instantaneous damping coefficient identification using a wavelet transform.

Stubbs et al. [16] first presented a damage localization method based on the decrease of strain energy obtained from the measured mode shapes of the structure [17]. This method has been applied to detect the damages in frame or truss structures such as bridges, buildings, and space structures. Cornwell et al. [18,19] extended this energy index concept to two-dimensional plate-like structures. The fractional strain energy of the plate before and after damage is used to define a damage index. This damage index identifies two edge cracks in an aluminum plate well. Choi et al. [20] utilized the changes in distributed modal compliance of the plate structure to detect the penetrated cracks in a steel plate. Recently, Hadjileontiadis and Duoka [21,22] developed an alternative method for detecting cracks in plates, based on fractal dimension (FD) analysis. The location of the crack can be determined by the abrupt changes in the spatial variation of a 2D-FD signal.

The current experimental achievements in both frame and plate structures are still limited to the detection of large or severe damage. Zou et al. [23] also indicated that the methods are unable to detect very small damage and require a large amount of data points for the further analysis of damage localization. Being a function of the second-order derivates of mode shape, the modal strain energy (MSE) is much more sensitive to the change of response than natural frequencies and mode shapes. It is therefore feasible to estimate small damage by using the change of MSE of the composite laminates before and after damage.

Hu et al. [24,25] adopted a differential quadrature method (DQM) to obtain the solution of modal strain energy, and successfully identified the location of surface cracks in various composite laminate plates, i.e. unidirectional fiber orientation, cross-ply, and quasi-isotropic laminates. The damage size of surface crack is relatively small in comparison to the previous studies. Furthermore, Hu et al. [26] effectively applied the same approach to the detection of damage in woven fabric composite laminates by adopting the equivalent cross-ply models to simulate its orthotropic behaviors.

The objective of this paper is to investigate the nondestructive detection of surface cracks in a woven laminate using a modal strain energy method (MSEM). A surface crack is created by using a knife to represent nominal damage which may include matrix cracks and fibre fracture. However, the surface crack which is comparatively small and does not significantly affect the global stiffness of the woven laminate. An equivalent cross-ply laminate model, an orthotropic model and a representative cell model are established to simulate the woven laminate. Using these three equivalent models, the unknown mechanical properties are obtained by using an inverse method combined with a finite element analysis. Consequently, the classical laminate theory is used to compute the modal strain energy. Using the change of MSE before and after damage, a damage index is defined to identify the location of surface crack. The quality and efficiency of measurement of this method may be improved by using optical methods such as laser Doppler vibrometer (LDV), which has been applied for vibration-based damage detection [27].

2. Experimental modal analysis

A woven fabric laminate is fabricated from the prepreg of (0/90) plain-weave carbon fibre cloths (F3T-282) and epoxy (DICY) in the form of ten-layer, nominally containing 63.7 % by volume of fibres. A hot-press machine is used to cure the prepreg. After curing, the laminate panel is cut to dimensions of 310 mm in length, 222 mm in width and 2.2 mm in thickness. A surface crack is created by using a knife and is located beside grid point numbers 66 and 81. The dimension of surface crack is about 16 mm in length and 1 mm in depth. The depth of the surface crack is obtained from measuring the fraction of knife tip cutting into the laminate.

Experimental modal analysis (EMA) is performed to obtain the modal displacement of the laminate before and after damage. The woven laminate is vertically hung by two cotton strings to simulate a completely free boundary condition. Fig. 1 shows the woven laminate and the arrangement of measured points. A mesh of 15×11 parallel grid points is employed in global detection as shown in Fig. 1(a). Since it is possible to detect the local area of the structure rather than measure the whole structure in practice, another finer arrangement of 7×7 parallel grid points is employed in local detection as shown in Fig. 1(b).

An impact hammer (PCB 086D80) with a force transducer is used to excite the woven laminate throughout the grid points. The sensitivity of the force transducer is 24.4 mV/N, and the dimension of the hammer tip is about 2.5 mm in diameter, which is close to the area of each grid point. The dynamic responses are measured by an accelerometer (PCB 352B10) fixed at the corner by using Petro-wax (PCB 080A109). The sensitivity of accelerometer is 9.57 mV/G. The weight of accelerometer is about 0.0015 kg which is small in comparison with the weight of woven laminate, i.e. 0.219 kg. The density of woven composite is directly measured from the woven laminate, i.e., $\rho = 1447$ kg/m^3.

A Siglab, Model 20–40, is used to record the frequency response functions (FRFs) between the measured acceleration and impact force. Each grid point is hit three times by impact hammer and the results of FRFs are automatically averaged by Siglab. ME'Scope, a software for general purpose curve fitting, is utilized to extract modal parameters, i.e., natural frequencies and mode shapes.

3. Finite element analysis and inverse method

Traditionally, mechanical properties of structure or component can be obtained from quasi-static tests. Strain gauges are generally used to measure the axial and lateral strains which are excellent for obtaining the mechanical properties. However, the properties obtained from local measurements may not be effective for representing the global behavior of woven laminates. To obtain the unknown mechanical properties, an inverse method is used to simulate the woven laminate by using finite element analysis (FEA). A commercial code ANSYS, which offers the function of design optimization, is employed to model the woven laminate. Akkerman [28] suggested a simplified approach of using an equivalent unidirectional cross-ply model to evaluate the bending stiffness of woven fabric laminate. In this study, three equivalent models, i.e. a cross-ply laminate model, an orthotropic model, and a representative cell (RC) model, are established by utilizing eight-node linear solid elements (SOLID46), which is more flexible for simulating surface cracks than plate and shell elements.

A cross-ply model is established by assigning laminae [0/90] for each element with different tensile moduli E_1 and E_2 in fiber and matrix directions as shown in Fig. 2(a). The orthotropic model is established by using the same cross-ply model with identical tensile moduli E_x and E_y in fiber and matrix directions. A normal mode analysis with completely free boundary condition is performed to obtain the natural frequencies and the associated

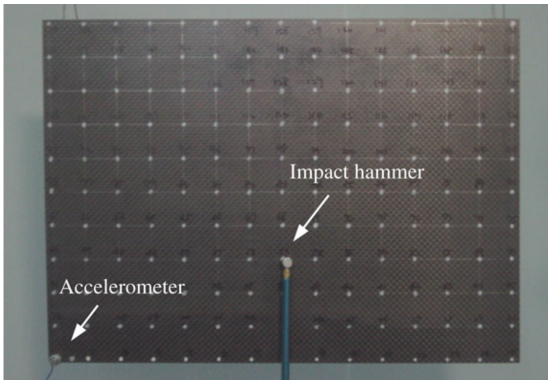

(a) Global testing.

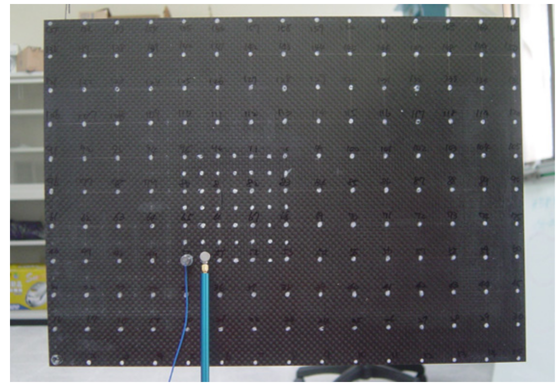

(b) Local testing.

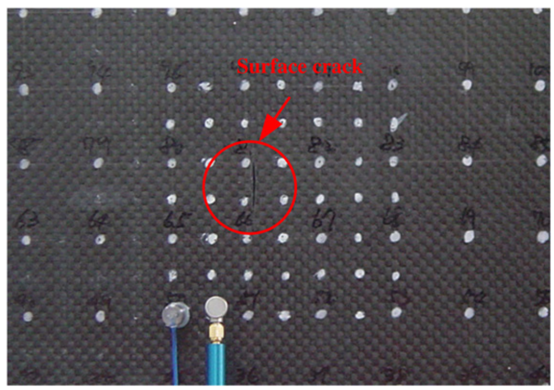

(c) Surface crack location.

Fig. 1. Woven laminate and measured points arrangement.

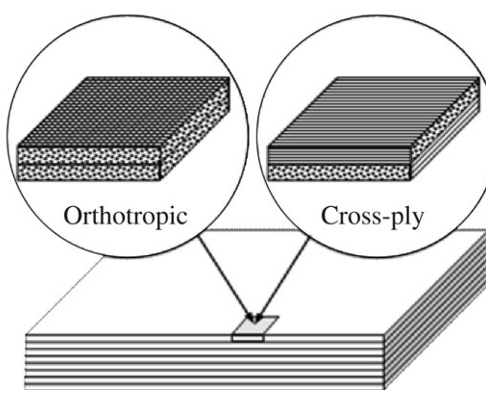

(a) Cross-ply & orthotropic models.

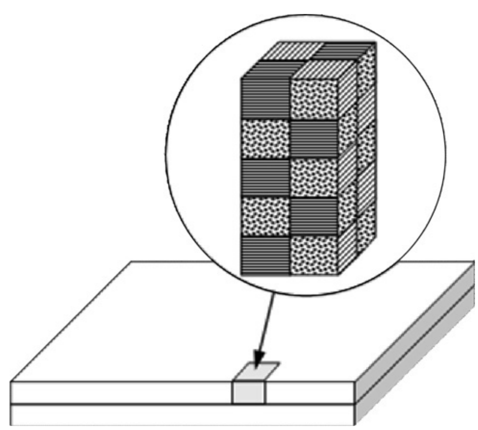

(b) Representative cell model.

Fig. 2. Illustration of three equivalent models.

mode shapes up to 2 kHz. A convergence study is performed to obtain a $42 \times 20 \times 8$ mesh model for equivalent cross-ply and orthotropic models, which is sufficient to solve the normal mode problem.

A unit RC model is established by assigning $[0/90]_5$ or $[90/0]_5$ for each element with different tensile moduli E_1 and E_2 in fiber and matrix directions. Thus, a representative cell consists of four solid elements as shown in Fig. 2(b), and a two-layer FE model consists of 34 410 elements. The mass effect of accelerometer is also considered in the FE model by assigning a mass element (MASS21) with 0.0015 kg to the laminate plate model. To simulate the surface crack, the corresponding nodes along the crack are separated.

The unknown mechanical properties of the woven laminate, are to be computed by using the subproblem approximation method, which is a zero-order optimization approach offered by ANSYS. It requires only the values of the dependent variables (objective function and state variables) and not their derivates. The dependent variables are first replaced with approximations by means of least squares fitting, and the constrained minimization problem is converted to an unconstrained problem using approximated functions. Minimization is then performed every iteration on the approximated function until convergence is achieved or termination is indicated. This method relies on approximation of the objective function and each state variable, a certain amount of data in the form of design sets is needed. The preliminary data can be directly generated by the user.

In cross-ply and RC models, the unknown mechanical properties are E_1, E_2, E_3, G_{12}, G_{13}, G_{23}, ν_{12}, ν_{13}, and ν_{23}. For unidirectional fibre-reinforced composites, the mechanical properties are basically identical in two matrix directions, i.e. $E_2 = E_3$, $G_{12} = G_{13}$, $\nu_{12} = \nu_{13}$. Besides, Hu et al. [25] indicates that the effect of shear modulus G_{23} and Poisson's ratio ν_{23} are not evident in thin composite laminate plates. Thus, the values of G_{23} and ν_{23} are assumed to be the same as G_{12} and ν_{12}. Consequently, the design variables for cross-ply and RC models are reduced to E_1, E_2, G_{12} and ν_{12}, respectively. Likewise, the design variables for the orthotropic model are reduced to E_x, G_{xy} and ν_{xy}. A state variable ζ is defined as the difference of natural frequencies obtained from FEA and EMA, i.e.

$$\zeta_n = \frac{f_n - \hat{f}_n}{\hat{f}_n} \tag{1}$$

where f_n and $\hat{f}_n$ denote the nth natural frequencies obtained from FEA and EMA, respectively. The state variable ζ_n is restricted within −0.1 and 0.1. The optimization process is the actual minimization of an objective function F which is given as

$$F(E_x, E_y, G_{xy}, \nu_{xy}) = \sum_{n=1}^{k} \zeta_n^2 \tag{2}$$

where k is the number of measured modes. Once an optimum set of design variables is obtained, the modal strain energy of the woven laminate can be computed.

4. Modal strain energy and damage index

The basic concept of the modal strain energy method is to use the change of modal strain energy due to the damage occurrence to define an index which can be used to identify the damage location in structure. The classical laminate plate theory for unidirectional fibre-reinforced composites is employed to compute the strain energy of woven laminate once the equivalent orthotropic material properties are obtained.

A laminate plate is subdivided into $N_x \times N_y$ sub-regions and denoting the location of each point by (x_i, y_j) as shown in Fig. 3, the strain energy during elastic deformation is given by

$$U = \frac{1}{2}\int_0^b\int_0^a \left[D_{11}\left(\frac{\partial^2 w}{\partial x^2}\right)^2 + D_{22}\left(\frac{\partial^2 w}{\partial y^2}\right)^2 + 2D_{12}\frac{\partial^2 w}{\partial x^2}\frac{\partial^2 w}{\partial y^2} + 4\left(D_{16}\frac{\partial^2 w}{\partial x^2} + D_{26}\frac{\partial^2 w}{\partial y^2}\right)\frac{\partial^2 w}{\partial x \partial y} + 4D_{66}\left(\frac{\partial^2 w}{\partial x \partial y}\right)^2\right]\mathrm{d}x\mathrm{d}y \tag{3}$$

where w is the transverse displacement and D_{ij} are the bending stiffness coefficients of the laminate. Considering a free vibration problem, for a particular normal mode, the total strain energy of the plate associated with mode shape displacement ϕ_k can be expressed as

$$U_k = \frac{1}{2}\int_0^b\int_0^a \left[D_{11}\left(\frac{\partial^2 \phi_k}{\partial x^2}\right)^2 + D_{22}\left(\frac{\partial^2 \phi_k}{\partial y^2}\right)^2 + 2D_{12}\frac{\partial^2 \phi_k}{\partial x^2}\frac{\partial^2 \phi}{\partial y^2} + 4\left(D_{16}\frac{\partial^2 \phi_k}{\partial x^2} + D_{26}\frac{\partial^2 \phi_k}{\partial y^2}\right)\frac{\partial^2 \phi_k}{\partial x \partial y} + 4D_{66}\left(\frac{\partial^2 \phi_k}{\partial x \partial y}\right)^2\right]\mathrm{d}x\mathrm{d}y. \tag{4}$$

Cornwell et al. [18] indicated that the change of strain energy in a sub-region may become significant if the damage is located at a single sub-region. Thus, the energy associated with sub-region (i, j) for the kth mode shape is given by

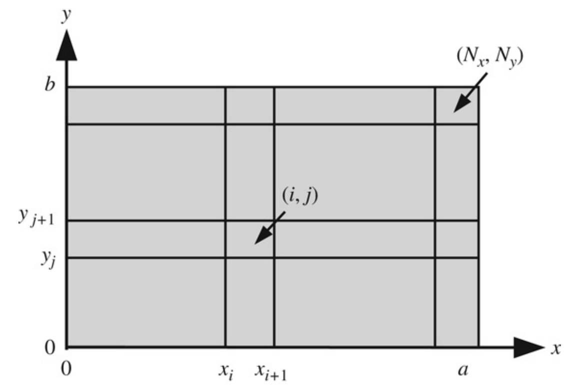

Fig. 3. A schematic illustrating of plate.

$$U_{k,ij} = \frac{1}{2}\int_{y_j}^{y_{j+1}}\int_{x_i}^{x_{i+1}} \left[D_{11}\left(\frac{\partial^2 \phi_k}{\partial x^2}\right)^2 + D_{22}\left(\frac{\partial^2 \phi_k}{\partial y^2}\right)^2 + 2D_{12}\left(\frac{\partial^2 \phi_k}{\partial x^2}\right)\left(\frac{\partial^2 \phi_k}{\partial y^2}\right) + 4\left(D_{16}\frac{\partial^2 \phi_k}{\partial x^2} + D_{26}\frac{\partial^2 \phi_k}{\partial y^2}\right)\left(\frac{\partial^2 \phi_k}{\partial x \partial y}\right) + 4D_{66}\left(\frac{\partial^2 \phi_k}{\partial x \partial y}\right)^2\right]\mathrm{d}x\mathrm{d}y. \tag{5}$$

Similarly, U_k^* and $U_{k,ij}^*$ represent the total strain energy and sub-regional strain energy of the kth mode shape ϕ_k^* for the damaged plate. The asterisk (*) denotes the damaged plate. The fractional energies of the undamaged and damaged plate are given by, respectively,

$$F_{k,ij} = \frac{U_{k,ij}}{U_k} \quad \text{and} \quad F_{k,ij}^* = \frac{U_{k,ij}^*}{U_k^*}. \tag{6}$$

Considering all measured mode shapes, m, the damage index in sub-region (i, j) is defined as

$$\beta_{ij} = \frac{\sum_{k=1}^{m} F_{k,ij}^*}{\sum_{k=1}^{m} F_{k,ij}}. \tag{7}$$

A normalized damage index is given by

$$Z_{ij} = \frac{\beta_{ij} - \bar{\beta}_{ij}}{\sigma_{ij}} \tag{8}$$

where $\bar{\beta}_{ij}$ and σ_{ij} represent the mean and standard deviation of the damage indices. Eq. (8) has been used to identify the damage location in unidirectional fibre-reinforced composite laminates. Once the mechanical behavior of woven laminates is replaced by the equivalent models, the above MESM can be effectively applied to woven laminate. An alternative numerical method DQM is introduced to solve the partial differential terms in strain energy formula.

5. Differential quadrature method

It is reported that the original DQM was first used in structural mechanics problems by Bert et al. [29]. This method is able to rapidly compute accurate solutions of partial differential equations

Table 1
Mechanical properties of the woven laminate.

Properties	Methods			
	Inverse method using FEA			Experiment
	$[0/90]_{ns}$	Orthotropic	RC	(Tensile test)
Tensile modulus (GPa)	$E_1 = 87.6$ $E_2 = 5.13$ $E_x = E_y = 47.9$	$E_x = E_y = 49.1$	$E_1 = 82.66$ $E_2 = E_3 = 12.3$ $E_x = E_y = 47.7$	$E_x = 57.8$ $E_y = 56.7$ $E_{ave} = 57.3$
Shear modulus (GPa)	$G_{12} = G_{xy} = 4.08$	$G_{xy} = 4.03$	$G_{12} = G_{xy} = 3.9$	$G_{xy} = 3.92$
Poisson's ratio	$\nu_{12} = 0.315$ $\nu_{xy} = 0.035$	$\nu_{xy} = 0.033$	$\nu_{12} = 0.214$ $\nu_{xy} = 0.06$	$\nu_{xy} = 0.042$

Table 2
Natural frequencies of the woven laminate (before damage).

ϕ_n	ω_n (Hz)						
	FEA			EMA	Difference (%)		
	$[0/90]_{ns}$	Orthotropic	RC		$[0/90]_{ns}$	Orthotropic	RC
(2, 2)	55.54	55.2	55.03	55.6	1.35	0.73	0.42
(3, 1)	142.7	135.2	133.1	133.8	6.73	1.12	−0.45
(3, 2)	178.9	172.9	171.2	174.0	3.53	0.06	−0.93
(1, 3)	229.5	256.3	258.2	256.3	−9.82	0.71	1.45
(2, 3)	253.1	276.8	278.9	278.4	−8.46	0.11	0.87
(3, 3)	347.3	356.4	354.5	361.3	−3.42	−0.89	−1.42
(4, 1)	395.2	377.9	373.7	370.2	6.90	2.22	1.08
(4, 2)	425.8	407.2	401.7	400.1	6.72	2.06	0.68

Table 3
Natural frequencies of the woven laminate (after damage).

ϕ_n	ω_n (Hz)						
	FEA			EMA	Difference (%)		
	$[0/90]_{ns}$	Orthotropic	RC		$[0/90]_{ns}$	Orthotropic	RC
(2, 2)	55.56	55.3	55.03	54.8	−0.13	−0.59	−1.08
(3, 1)	142.6	135.1	133.0	133.7	6.58	0.97	−0.60
(3, 2)	179.0	173.0	171.1	172.8	2.87	−0.57	−1.67
(1, 3)	229.5	256.3	258.1	254.5	−10.5	0.00	0.70
(2, 3)	253.1	276.8	278.8	276.5	−9.09	−0.57	0.14
(3, 3)	347.3	356.4	354.3	359.6	−3.87	−1.36	−1.94
(4, 1)	394.7	377.5	373.1	369.7	6.62	1.97	0.78
(4, 2)	425.8	407.2	401.4	399.0	6.42	1.77	0.32

by using only a few grid points in the respective solution domains [30]. The basic idea of DQM is to approximate the partial derivatives of a function $f(x_i, y_j)$ with respect to a spatial variable at any discrete point as the weighted linear sum of the function values at all the discrete points chosen in the solution domain of spatial variable. This can be expressed mathematically as

$$f_x^{(n)}(x_i, y_j) = \sum_{r=1}^{N_x} C_{ir}^{(n)} f(x_r, y_j) \tag{9}$$

$$f_y^{(m)}(x_i, y_j) = \sum_{s=1}^{N_y} \overline{C}_{js}^{(m)} f(x_i, y_s) \tag{10}$$

$$f_{xy}^{(n+m)}(x_i, y_j) = \sum_{r=1}^{N_x} C_{ir}^{(n)} \sum_{s=1}^{N_y} \overline{C}_{js}^{(m)} f(x_r, y_s) \tag{11}$$

where $i = 1, 2, \ldots, N_x$ and $j = 1, 2, \ldots, N_y$ are the grid points in the solution domain having $N_x \times N_y$ discrete number of points. $C_{ir}^{(n)}$ and $\bar{C}_{js}^{(m)}$ are the weighting coefficients associated with the nth order and the mth order partial derivatives of $f(x_i, y_j)$ with respect to x and y at the discrete point (x_i, y_j) and $n = 1, 2, \ldots, N_x - 1$, $m = 1, 2, \ldots, N_y - 1$. The weighting coefficients can be obtained using the following recurrence formulae

$$C_{ir}^{(n)} = n\left(C_{ii}^{(n-1)} C_{ir}^{(1)} - \frac{C_{ir}^{(n-1)}}{x_i - x_r}\right)$$

$$i, r = 1, 2, \ldots, N_x \text{ but } r \neq i;\ n = 2, 3, \ldots, N_x - 1 \tag{12}$$

$$\overline{C}_{js}^{(m)} = n\left(\overline{C}_{jj}^{(m-1)} \overline{C}_{js}^{(1)} - \frac{\overline{C}_{js}^{(n-1)}}{y_j - y_s}\right)$$

$$j, s = 1, 2, \ldots, N_y \text{ but } s \neq j;\ m = 2, 3, \ldots, N_y - 1 \tag{13}$$

where

$$C_{ii}^{(n)} = -\sum_{r=1, r\neq i}^{N_x} C_{ir}^{(n)};$$

$$i = 1, 2, \ldots, N_x, \text{ and } n = 1, 2, \ldots, N_x - 1 \tag{14}$$

$$\overline{C}_{jj}^{(m)} = -\sum_{s=1, s\neq j}^{N_y} \overline{C}_{js}^{(m)};$$

$$j = 1, 2, \ldots, N_y, \text{ and } m = 1, 2, \ldots, N_y - 1 \tag{15}$$

$$C_{ir}^{(1)} = \frac{M^{(1)}(x_i)}{(x_i - x_r) M^{(1)}(x_r)}; \quad i, r = 1, 2, \ldots, N_x, \text{ but } r \neq i \tag{16}$$

$$\overline{C}_{js}^{(1)} = \frac{P^{(1)}(y_j)}{(y_j - y_s) P^{(1)}(y_s)}; \quad j, s = 1, 2, \ldots, N_y, \text{ but } s \neq j \tag{17}$$

where

$$M^{(1)}(x_i) = \prod_{r=1, r\neq i}^{N_x} (x_i - x_r) \quad \text{and} \quad P^{(1)}(y_j) = \prod_{s=1, s\neq j}^{N_y} (y_j - y_s).$$

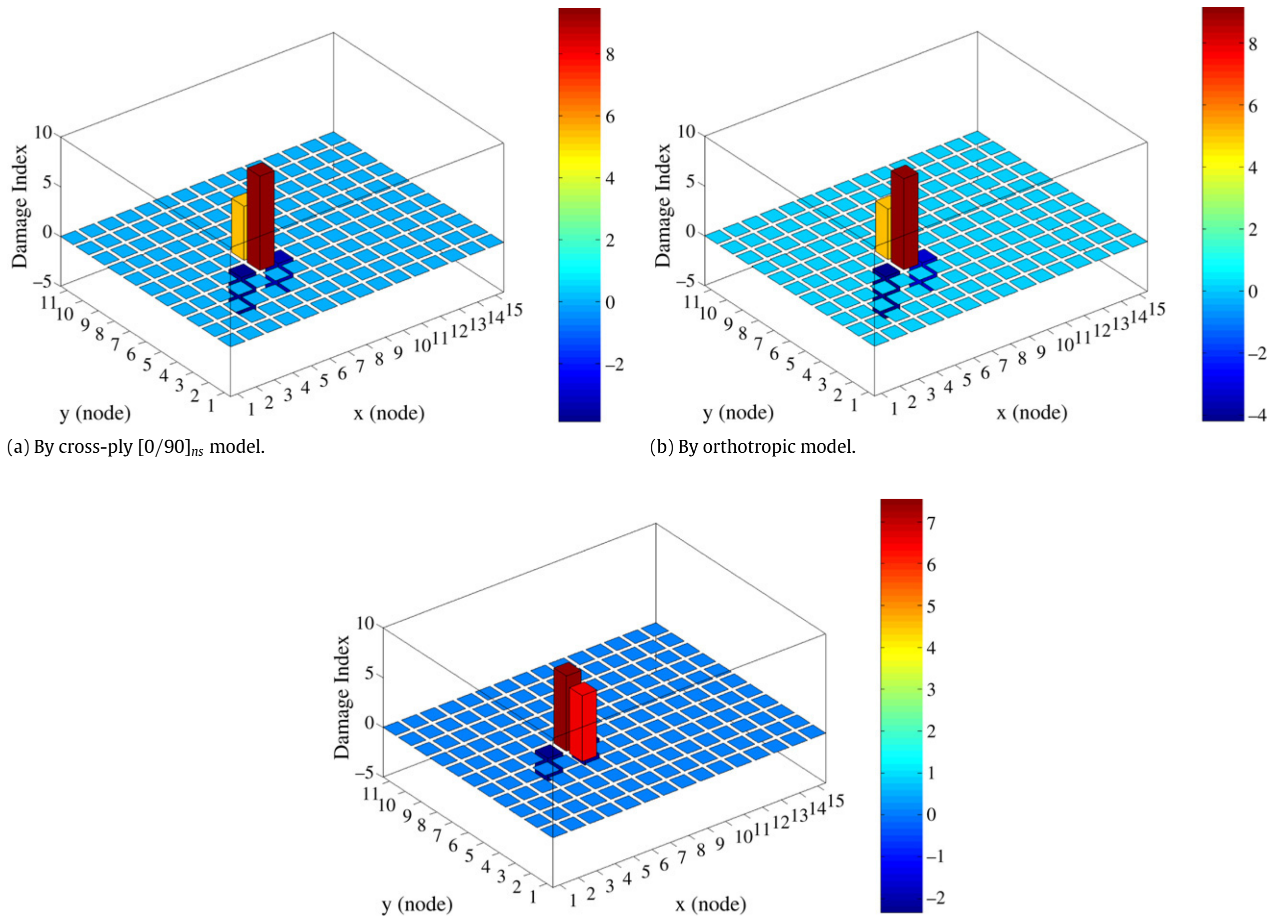

(a) By cross-ply $[0/90]_{ns}$ model.

(b) By orthotropic model.

(c) By RC model.

Fig. 4. Damage detection by FEA.

The above equations are applied to compute the strain energy once the kth mode shape $\phi_{k,ij} = f_k(x_i, y_j)$ is obtained.

6. Results and discussion

6.1. Model verification

The unknown mechanical properties obtained from the inverse method are validated by using EMA. Moreover, tensile tests are also performed to measure the mechanical properties for comparison. Two coupon specimens are cut from the woven laminate at different locations with perpendicular directions x and y. Strain gauges are then used to measure the axial and lateral deformations. Thus, the tensile modulus and Poisson's ratio are obtained from the average of test data E_x and E_y. To test the shear modulus G_{xy}, another coupon specimen is cut from the woven laminate at the direction of 45-degree. Since the mechanical behaviors of woven laminate are similar to cross-ply or orthotropic laminates, the 45-degree specimen cut from the woven laminate should be equivalent to the specimen cut from a ± 45-degree continuous fibre-reinforced composite laminate. The shear modulus is therefore computed by using the classical laminate theory, i.e.

$$G_{xy} = \frac{\sigma_o}{2(\varepsilon_x - \varepsilon_y)} \tag{18}$$

where σ_o is applied stress; ε_x and ε_y are measured strains in axial and lateral directions of the specimens.

Table 1 lists the mechanical properties of woven laminate. The data show that tensile modulus E_x and E_y and shear modulus G_{xy} obtained from three equivalent models are very much alike except for the Poisson's ratio. The mechanical properties obtained from tensile tests show about 14%–17% deviation in tensile modulus from those of by inverse method. However, the shear modulus is almost identical to those of by inverse method. The outcome shows that the mechanical properties obtained from local measurement may not be satisfactory to represent the global mechanical behaviors of woven laminate.

Table 2 lists the first eight natural frequencies and mode shapes of the woven laminate before damage. The small difference between the natural frequencies of FEA and EMA demonstrate that three equivalent models are reliable to simulate woven laminate in free vibration problems. Nevertheless, the orthotropic model seems to serve a slightly better simulation than the other two models. It is also found that the cross-ply model and the RC model are more sensitive to the initial values of design variables in the optimization process than the equivalent orthotropic model.

Table 3 lists the first eight natural frequencies and mode shapes of the woven laminate after damage. The data show that natural frequencies are almost the same as those in Table 2. Moreover, the first eight mode shape contours as shown in Table 4 demonstrate that the mode shapes obtained from both FEA and EMA are almost identical. This approach benefits us to capably characterize the unknown mechanical properties of a woven laminate without making any coupon specimens. Unfortunately, experimental data show that the natural frequencies and the associate mode shapes of woven laminates before and after damage are almost equal. In fact, it is not easy to detect the damage in a woven laminate by using the change of natural frequencies and mode shapes, not to mention the identification of damage location. Accordingly, the damage index developed by the MSEM is therefore significant.

Table 4
Mode shape of the woven laminate.

Mode	EMA	$[0/90]_{ns}$	Orthotropic	RC
(2, 2)	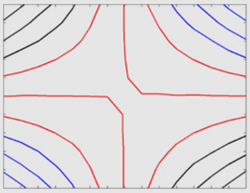			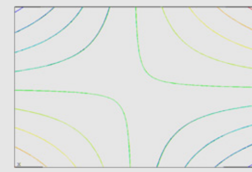
(3, 1)	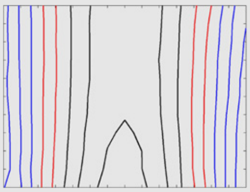	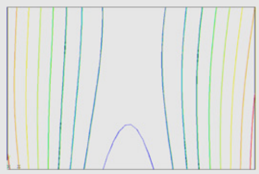	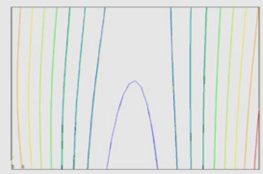	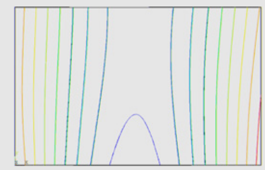
(3, 2)	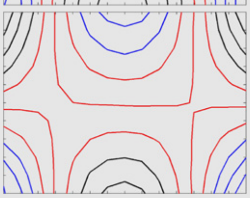	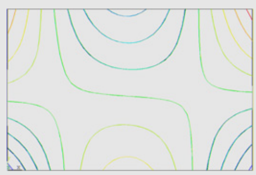	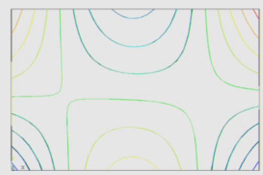	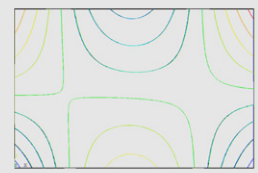
(1, 3)	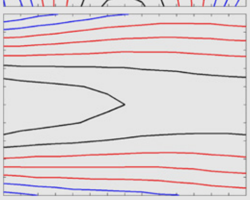	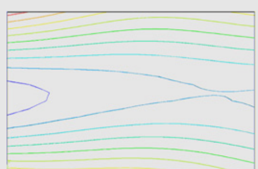	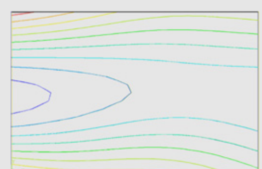	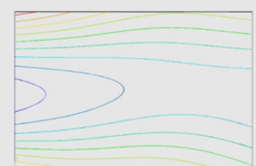
(2, 3)	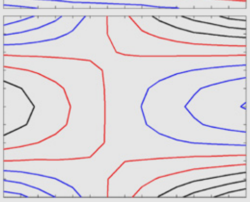	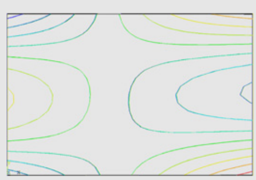	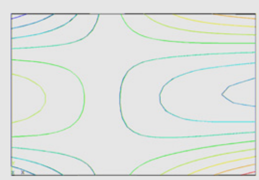	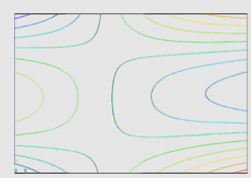
(3, 3)	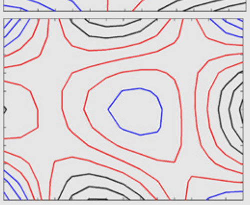	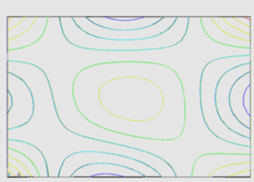	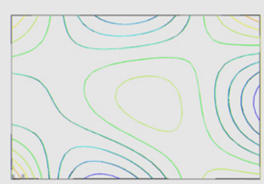	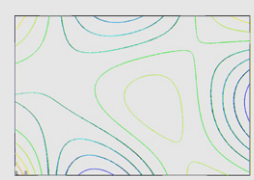
(4, 1)	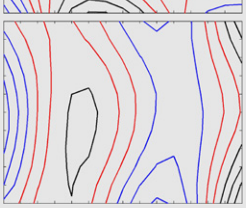	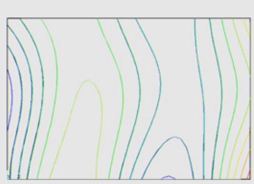	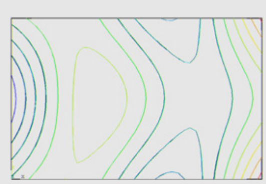	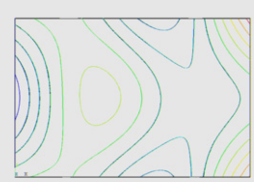
(4, 2)	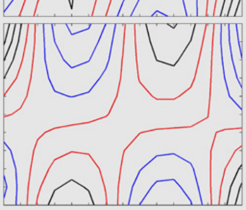	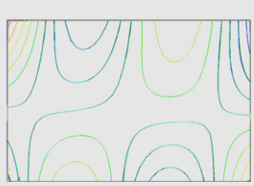	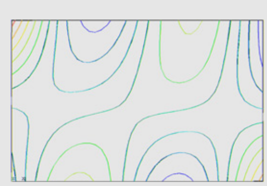	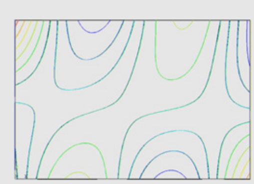

6.2. *Detection of surface crack*

A damage index is used to identify the location of surface crack in a woven laminate. FEA is first used to evaluate this approach. Fig. 4 shows the detection results of FEA through the three equivalent models. The peak values of the damage index successfully identify the location of surface cracks. Only the first four mode shapes are used to compute the modal strain energy and damage index in this analysis. The encouraging outcome of good identification of surface crack leads to the following experimental results.

Four tests, i.e. two of global detection and two of local detection, are performed for the damage detection of EMA. The damage indices using the first five, six, seven, and eight measured mode

Table 5
Global damage detection of EMA (by cross-ply $[0/90]_{ns}$ model).

No. of modes	Damage location	1st measurement	2nd measurement
8	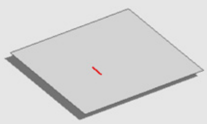	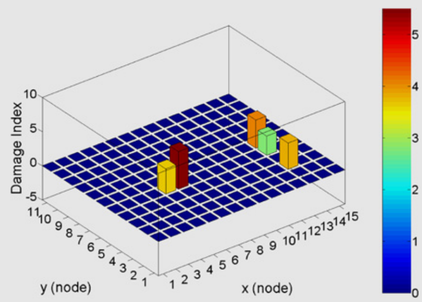	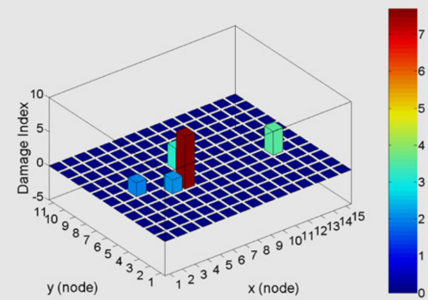
7	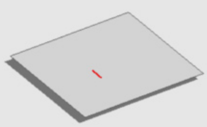	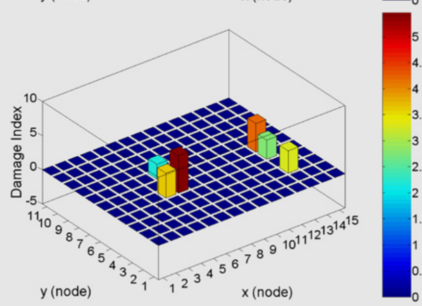	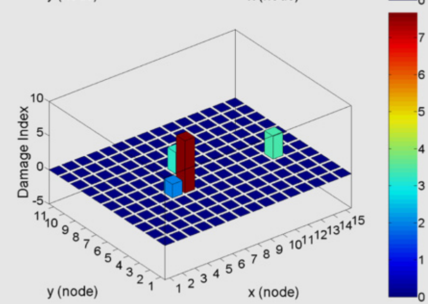
6	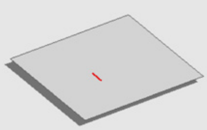	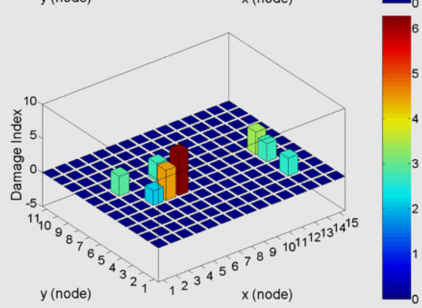	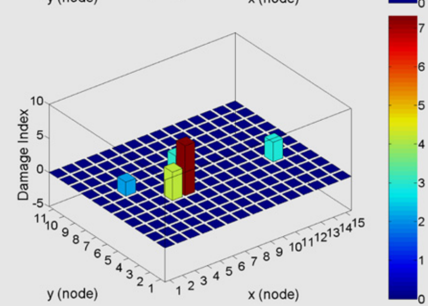
5	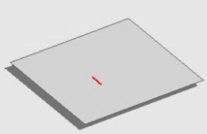	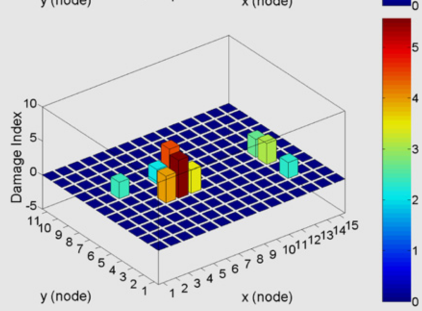	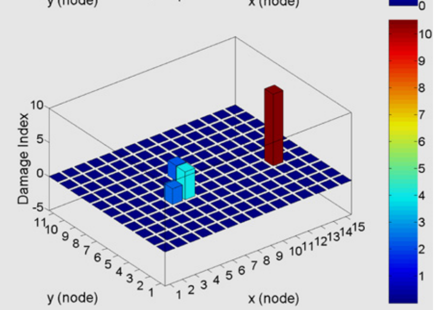
4	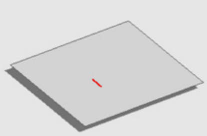	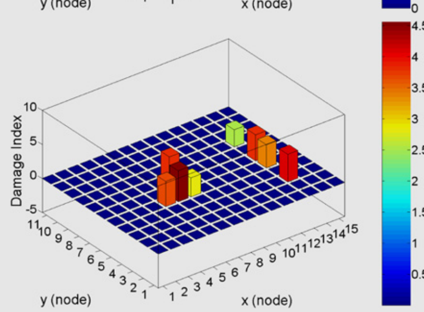	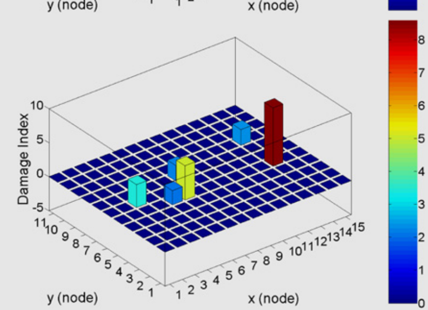

shapes of the woven laminate are investigated. Cornwell et al. [18] suggested that a damage index with value greater than two is associated with potential damage locations. Thus, the values of damage index less than two are truncated in this study. Table 5 shows the two measurements of global detection through equivalent cross-ply model. The use of first four, five, six, seven and eight mode shapes is investigated. The detection result in first measurement exhibits more scatter than those of in the second measurement. However, the peak value of damage index in both measurements successfully identifies the surface crack location, though some scatter emerges at undamaged areas. In general, the higher resolution of damage index will be obtained if more measured mode shapes are used in the computation of strain energy and damage index. The experimental results show that

Table 6
Global damage detection of EMA (by orthotropic model).

<table>
<tr><th>No. of modes</th><th>Damage location</th><th>1st measurement</th><th>2nd measurement</th></tr>
<tr><td>8</td><td>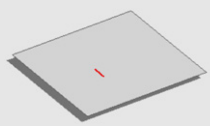</td><td>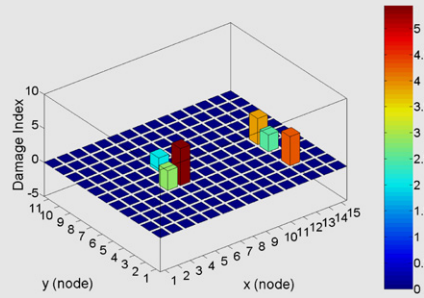
</td><td>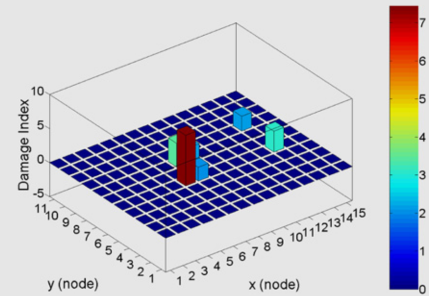
</td></tr>
<tr><td>7</td><td>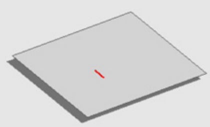</td><td>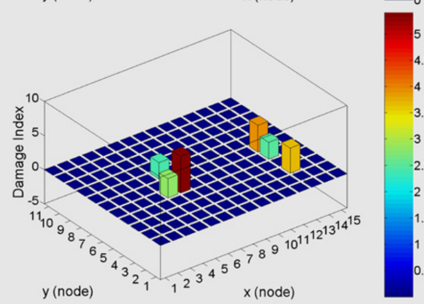
</td><td>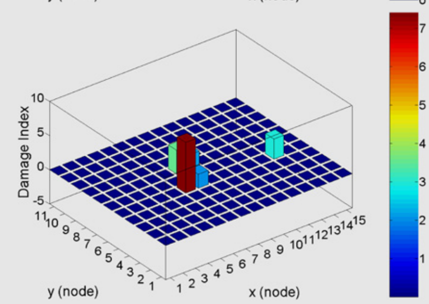
</td></tr>
<tr><td>6</td><td>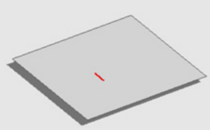</td><td>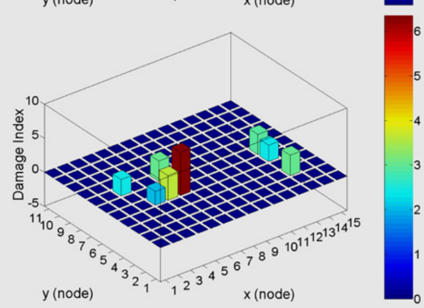
</td><td>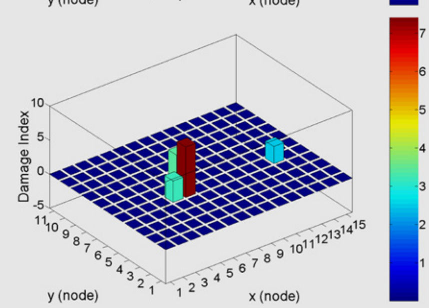
</td></tr>
<tr><td>5</td><td>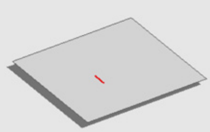</td><td>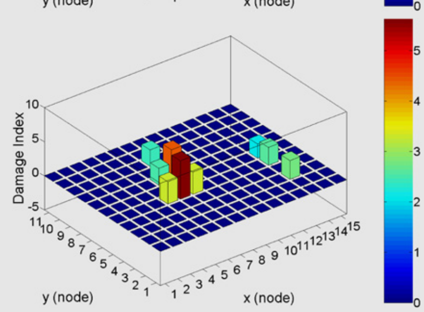
</td><td>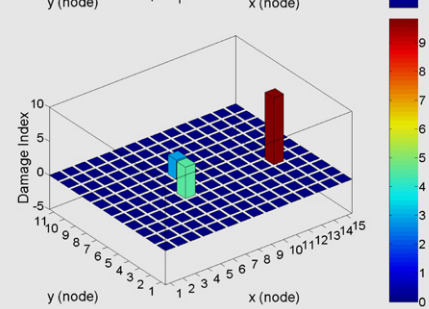
</td></tr>
<tr><td>4</td><td>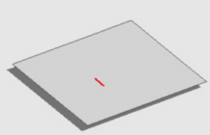</td><td>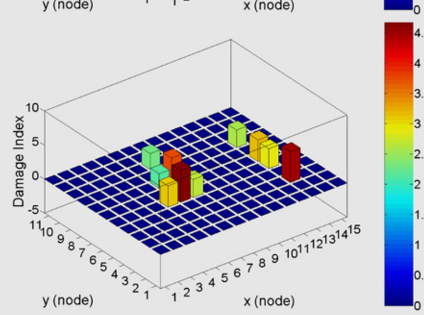
</td><td>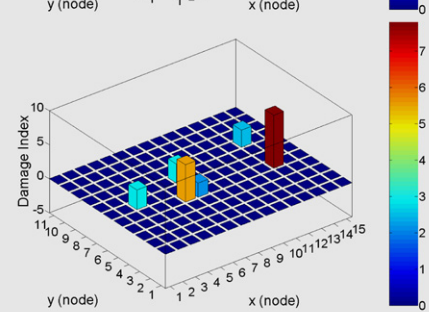
</td></tr>
</table>

the damage area is accurately detected when using the first eight, seven, or six mode shapes, but detections are false as the first five or four mode shapes are used in the second measurement.

Tables 6 and 7 show similar results through the orthotropic and RC models, respectively. It looks as if the damage indices obtained from those three equivalent models are very much alike; however, the data values in those three detections are indeed a little different from one another. Apparently, the global detection results through the three equivalent models successfully identify surface crack location. The first six measured mode shapes are required at least to compute the strain energy and damage index.

It is noticeable that the scatter of the damage index in undamaged areas, i.e. (13, 3), (13, 5) and (13, 6), are almost the same and shown in the first measurement of the three equivalent models. After checking the test data, the coherences of the frequency response functions obtained from those measured

Table 7
Global damage detection of EMA (by RC model).

No. of modes	Damage location	1st measurement	2nd measurement
8	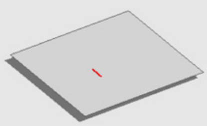	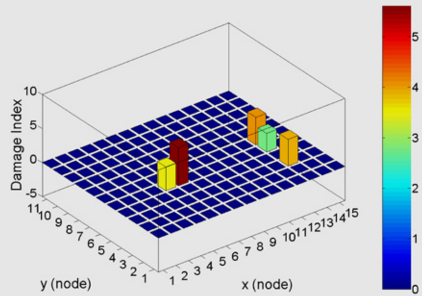	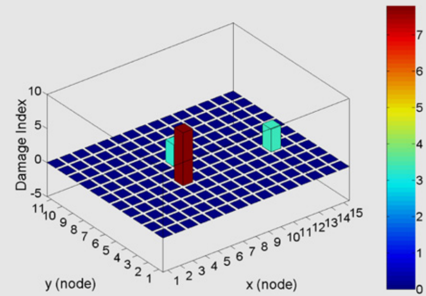
7	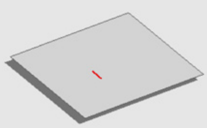	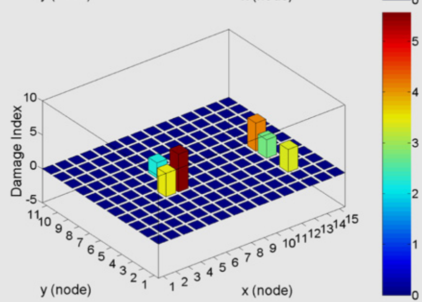	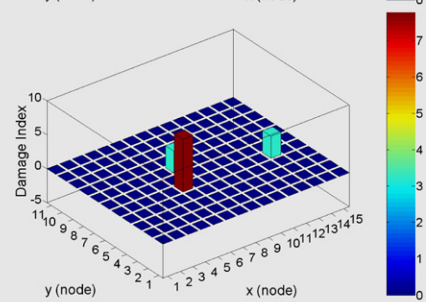
6	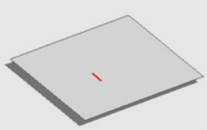	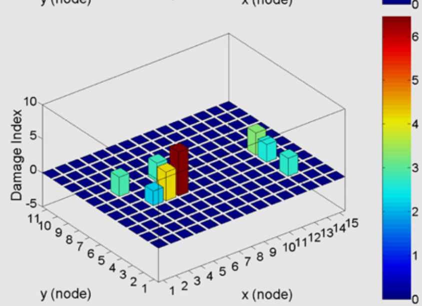	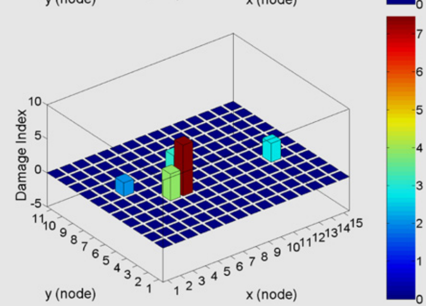
5	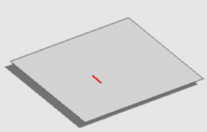	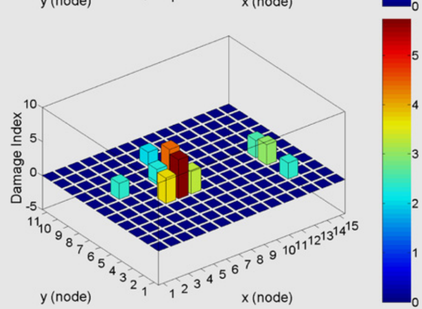	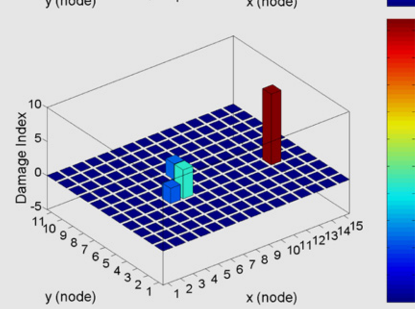
4	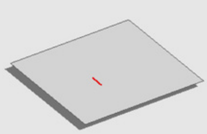	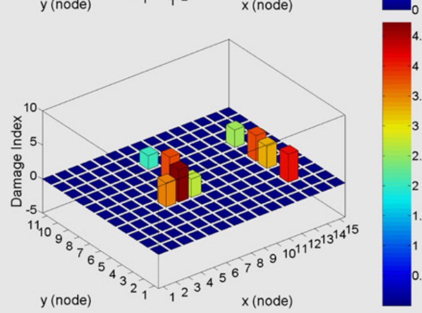	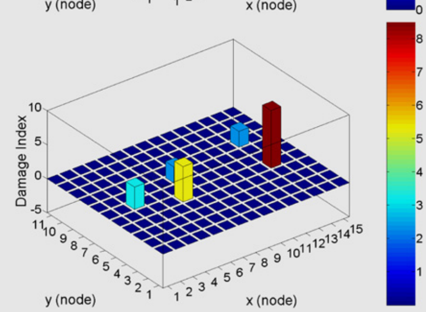

points are worse than others in the first measurement. The test results in second measurement seem to be improved. In fact, the accidental poor measurement always causes scatter of damage index especially when the experiment is performed by hand.

In practical applications, structural health can be monitored throughout its service life. The summation of damage indices measured at different times may magnify the signal of damage and even balance out the scatter in undamaged areas [25]. For instance, the summation of damage indices obtained from the two measurements shown in Tables 5–7 will enhance the damage indices at the surface crack location.

Since global detection may result in a large amount of measured points, it is possible to detect local areas of the structure rather than the whole structure in practice. Another two tests of the local detection were performed to investigate the sensitivity of area and grid point number of measurement. The detection area is reduced

Table 8
Local damage detection of EMA (by cross-ply $[0/90]_{ns}$ model).

No. of modes	Damage location	1st measurement	2nd measurement
8	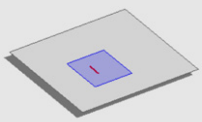	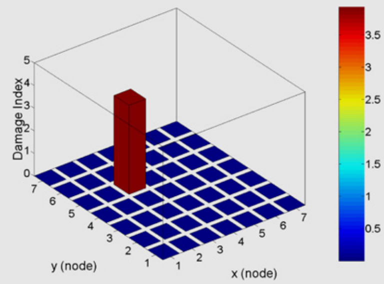	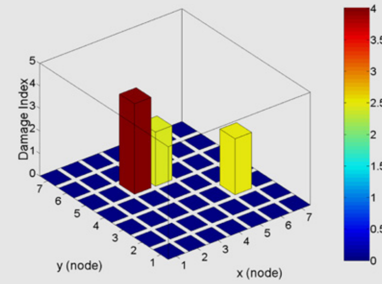
7	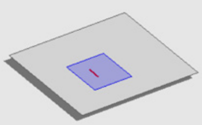	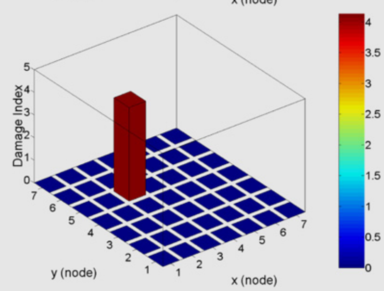	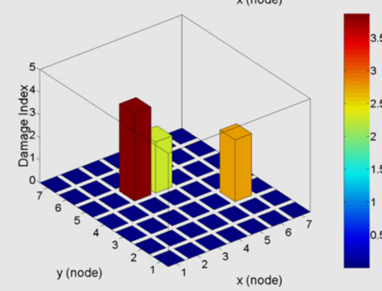
6	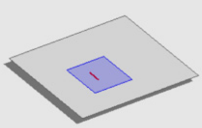	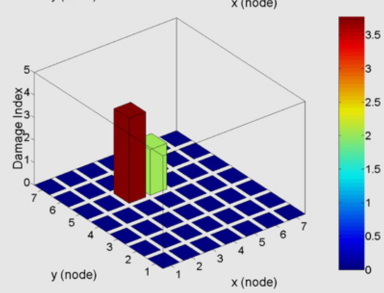	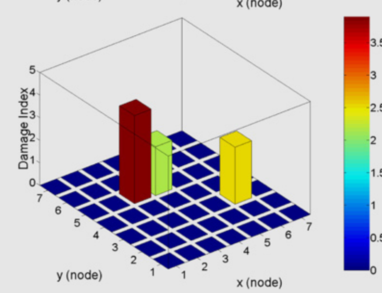
5	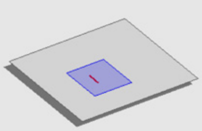	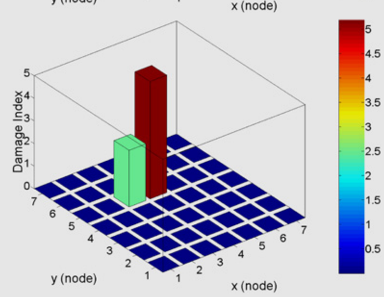	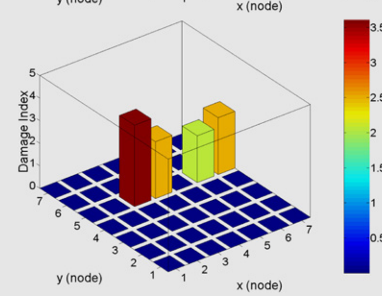
4	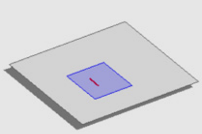	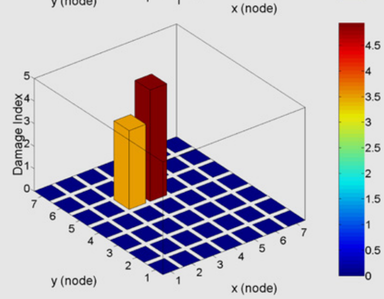	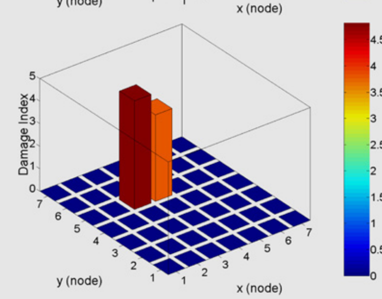
3	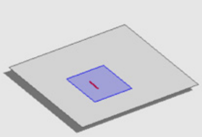	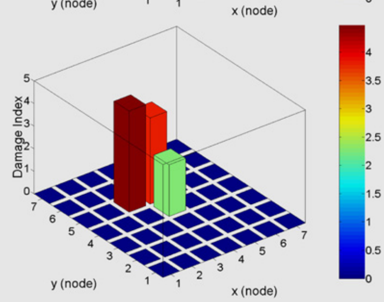	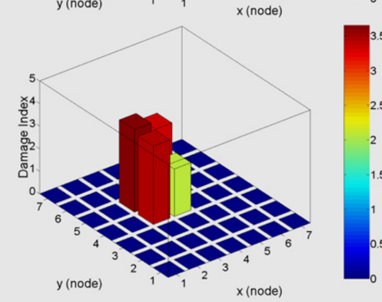

Table 9
Local damage detection of EMA (by orthotropic model).

No. of modes	Damage location	1st measurement	2nd measurement
8	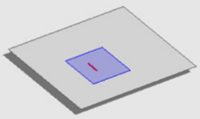	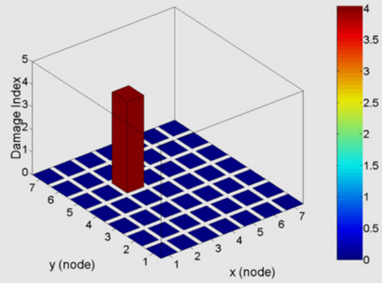	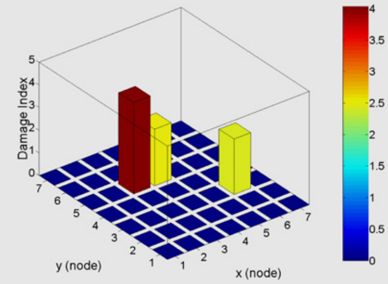
7	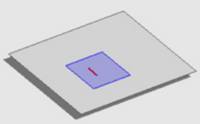	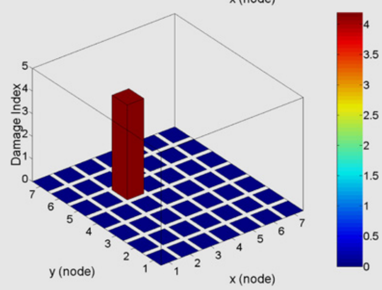	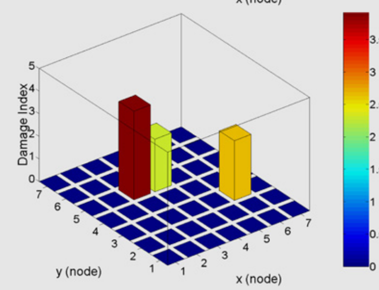
6	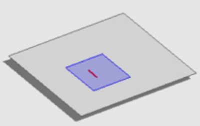	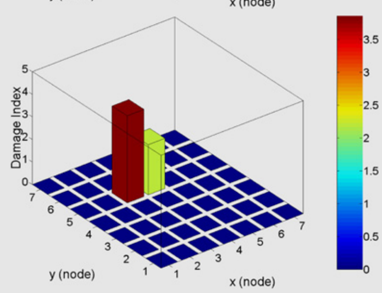	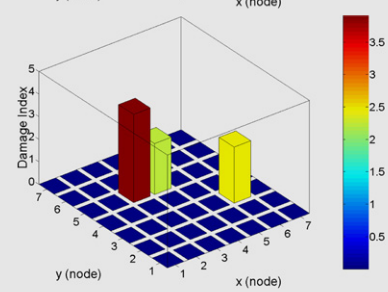
5	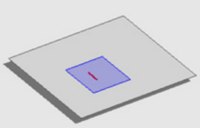	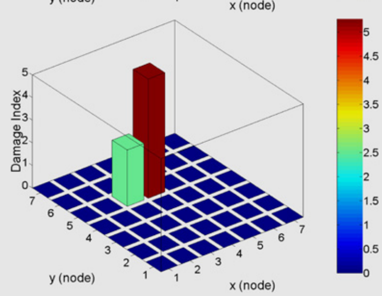	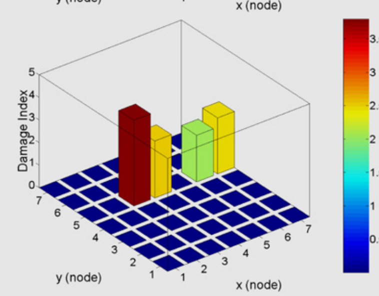
4	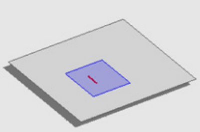	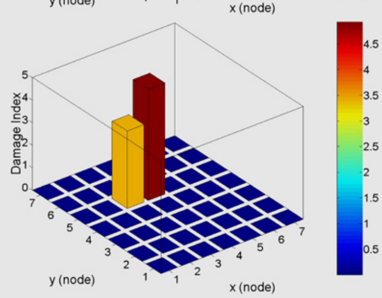	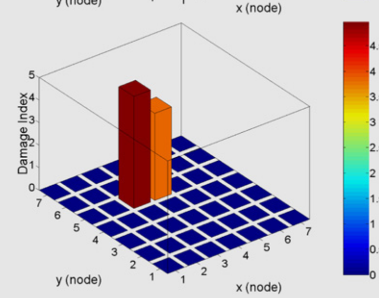
3	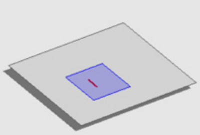	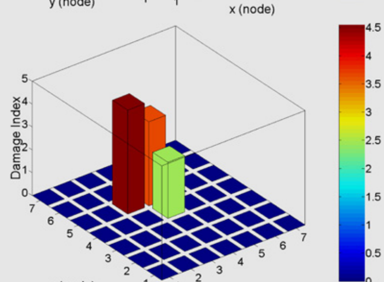	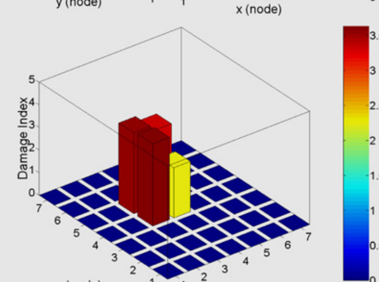

Table 10
Local damage detection of EMA (by RC model).

No. of modes	Damage location	1st measurement	2nd measurement
8	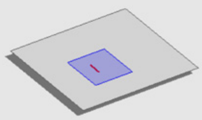	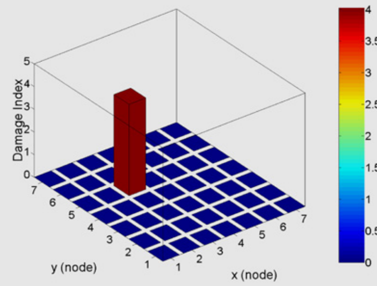	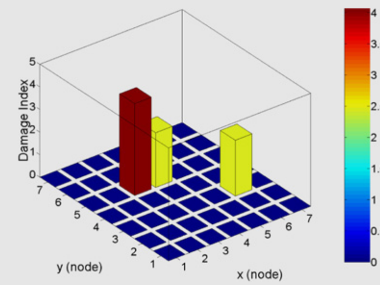
7	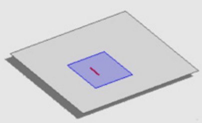	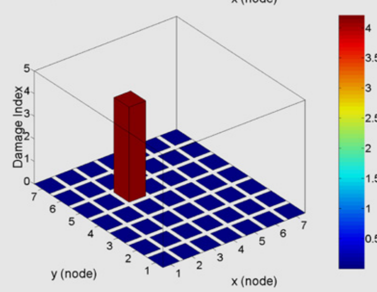	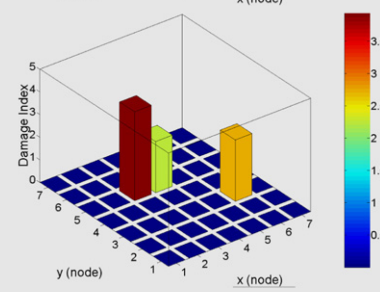
6	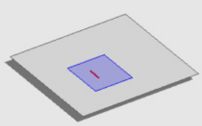	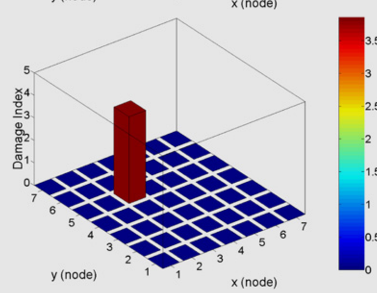	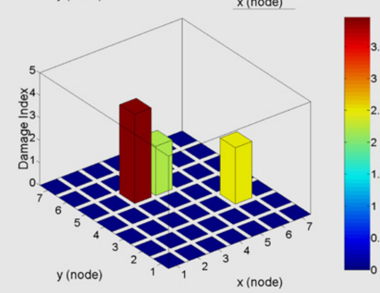
5	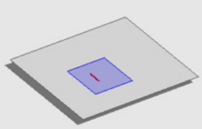	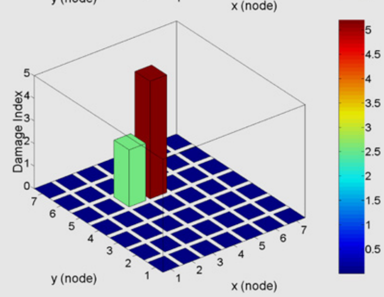	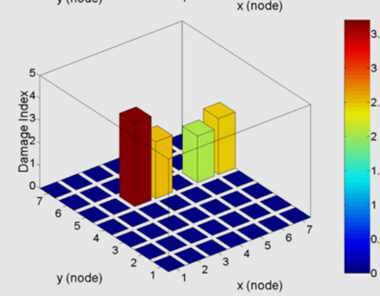
4	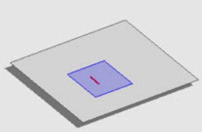	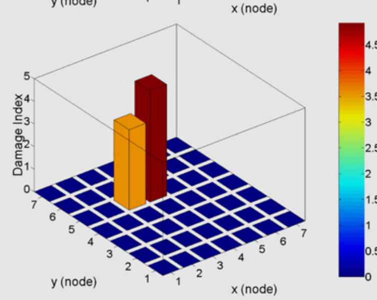	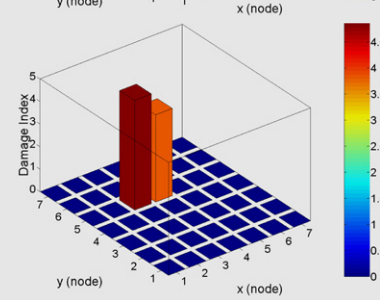
3	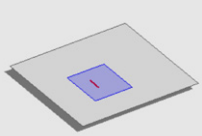	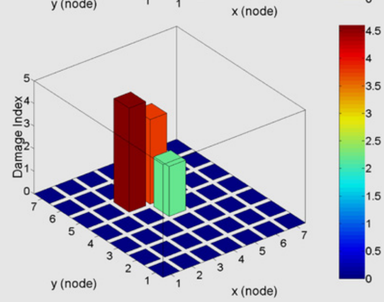	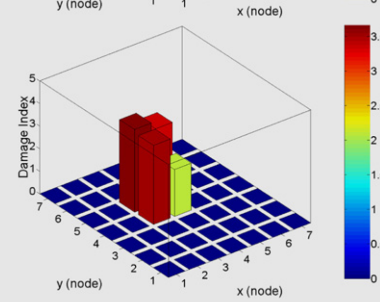

to 7 × 7 measured points as shown in Fig. 2(b). Similarly, some of the first measured mode shapes obtained from EMA are adopted to compute the strain energy and damage index.

Tables 8–10 show the two measurements of local detection through the three equivalent models. The use of first three, four, five, six, seven and eight mode shapes is also investigated. The detection results of the three equivalent models look very similar. In the first measurement, only one peak of damage index clearly appears at the location of surface crack as the first eight or seven mode shapes are used to compute the damage index. By using the first six, five or four mode shapes, two peaks of damage index also identify the surface crack location well. Even when only the first three mode shapes are used, three peaks of damage index still reveal the surface crack location.

The detection results in second measurement exhibit more scatter; however, the damage indices also well identify the surface crack location. Overall, the experimental results demonstrate that the MSEM is good enough in the identification of surface crack in woven laminate.

7. Conclusions

The detection of a surface crack in a woven laminate using MSEM has been investigated. The mechanical behavior of a woven laminate is reliably simulated by three equivalent models, i.e. the cross-ply model, the orthotropic model and the representative cell model. Its unknown mechanical properties are successfully estimated by using an inverse method through the equivalent models. The damage indices obtained from the three equivalent models properly identify the surface crack location in both global and local detections of woven laminate. Only a few measured mode shapes of the woven laminate before and after damage are required in this approach. The challenge of this method still lies in the accuracy of measurement and limitation of grid point numbers. Although the experimental tools used in this study are time consuming and the measurement may be not good enough, the preliminary achievement of MSEM in the damage detection of woven laminate is presented. It is practicable to obtain more promising results by employing more advanced test equipment. The limitations and applicability to different types and different levels of damage in woven fabric composites are still to be validated in future work.

References

[1] Naik NK, Shembekhar PS. Elastic behavior of woven fabric composites: III—Laminate design. J Compos Mater 1992;26:2522–41.
[2] Chen B, Chou TW. Free vibration analysis of orthogonal-woven fabric composites. Compos A 1999;30:285–97.
[3] Woo K, Whitcomb JD. Global/local finite element analysis for textile composites. J Compos Mater 1994;28:1305–20.
[4] Whitcomb JD, Kondagunta G, Woo K. Boundary effects in woven composites. J Compos Mater 1995;29:507–24.
[5] Woo K, Whitcomb JD. Three-dimensional failure analysis of plain weave textile composites using a global/local finite element method. J Compos Mater 1996; 30:984–1003.
[6] Le Pagea BH, Guildb FJ, Ogina SL, Smith PA. Finite element simulation of woven fabric composites. Compos A 2004;35:861–72.
[7] Gao F. Damage accumulation in woven-fabric CFRP laminates under tensile loading: Part 1. Observations of damage accumulation. Compos Sci Tech 1999; 59:123–36.
[8] Cawley P, Adams RD. The location of defects in structure from measurements of natural frequencies. J Strain Anal 1979;14:49–57.
[9] Tracy JJ, Pardoen GC. Effect of delamination on the natural frequencies of composite laminates. J Comp Mater 1989;23:1200–15.
[10] Salawu OS, Williams C. A review of full-scale dynamic testing of bridge structures. Eng Struct 1995;17:113–21.
[11] Salawu OS. Detection of structural damage through changes in natural frequency: A review. Eng Struct 1997;19:718–23.
[12] Shen MHH, Grady JE. Free vibration of delaminated beams. AIAA J 1992;30: 1361–70.
[13] Kim JT, Ryu YS, Chp HM, Stubbs N. Damage identification in beam-type structures: Frequency-based method vs. mode-shape-based method. Eng Struct 2003;25:57–67.
[14] Kim JT, Park JH, Lee BJ. Vibration-based damage monitoring in model plate-girder bridges under uncertain temperature conditions. Eng Struct 2007;29: 1354–65.
[15] Curadelli RO, Riera JD, Ambrosins D, Amani MG. Damage detection by means of structural damping identification. Eng Struct 2008;30:3497–504.
[16] Stubbs N, Kim JT, Topole K. An efficient and robust algorithm for damage localization in offshore platforms. Proc ASCE Tenth Struct Cong 1992;543–6.
[17] Stubbs N, Kim JT, Farrar CR. Field verification of a non-destructive damage localization and severity estimation algorithm. In: Proc 13th Int Modal Anal Conf. 1995. p. 210–8.
[18] Cornwell PJ, Dobeling SW, Farrar CR. Application of the strain energy damage detection method to plate-like structures, In: Proc 15th Int Modal Anal Conf 1997. p. 1312–8.
[19] Cornwell PJ, Dobeling SW, Farrar CR. Application of the strain energy damage detection method to plate-like structures. J Sound Vib 1999;224(2):359–74.
[20] Choi S, Park P, Yoon S, Stubbs N. Nondestructive damage identification in plate structures using changes in modal compliance. NDT&E Internat 2005; 38:529–40.
[21] Hadjileontiadis LJ, Douka E. Crack detection in plates using fractal dimension. Eng Struct 2007;29:1612–25.
[22] Hadjileontiadis LJ, Douka E. Kurtosis analysis for crack detection in thin isotropic rectangular plates. Eng Struct 2007;29:2353–64.
[23] Zou Y, Tong L, Steven GP. Vibration-based model-dependent damage (Delamination) identification and health monitoring for composite structures—A review. J Sound Vib 2000;2:357–78.
[24] Hu H, Wang BT, Lee CH. Damage detection of surface crack in composite quasi-isotropic laminate using modal analysis and strain energy method. Key Eng Mater 2006;306–308:757–62.
[25] Hu H, Wang BT, Lee CH, Su JS. Damage detection of surface cracks in composite laminates using modal analysis and strain energy method. Compos Struct 2006;74:399–405.
[26] Hu H, Wang J, Jwo SL. A damage index to detect surface cracks in woven fabric composite laminates using experimental modal analysis, in: The 21st Annual Technical Conference of the American Society for Composites. Paper no. 161. 2006.
[27] Siringoringo DM, Fujino Y. Experimental study of laser Doppler vibrometer and ambient vibration for vibration-based damage detection. Eng Struct 2006;28: 1803–15.
[28] Akkerman R. Laminate mechanics for balanced woven fabrics. Compos B 2006; 37:108–16.
[29] Bert CW, Jang SK, Striz AG. Two new approximate methods for analyzing free vibration of structural components. AIAA J 1988;26:612–8.
[30] Bellman RE, Kashef KG, Casti J. Differential quadrature: A technique for the rapid solution of nonlinear partial differential equation. J Comput Phys 1972; 10:40–52.